http://dx.doi.org/10.5012/bkcs.2013.34.12.3895

Analytical and Numerical Calculations of Diffusion Effects on the Intermolecular Multiple Quantum Coherences in Solution NMR

Kee-Choo Chung,[†] Gyungsu Jin,[†,‡] Daeun Won,[†] Su Jung Hwang,[‡] Jee-Hyun Cho,[‡] Suk-Kyu Chang,[†] and Sangdoo Ahn[†,*]

[†]*Department of Chemistry, Chung-Ang University, Seoul 156-756, Korea.* [*]*E-mail: sangdoo@cau.ac.kr*
[‡]*Division of Magnetic Resonance Research, Korea Basic Science Institute, Ochang 363-883, Korea*
Received September 7, 2013, Accepted September 21, 2013

Key Words : NMR, Distant dipolar field, iMQC, Diffusion, Bloch equation

The intermolecular multiple quantum coherences (iMQCs) that are generated by intermolecular dipolar interactions between distant spins on different molecules, have recently gained considerable attention because their properties are intrinsically different from those of conventional single quantum coherences (SQCs) in solution NMR.[1-12] This feature allows for a wider range of applications in NMR and MR imaging.[7-12]

Signal attenuation behaviors of the iMQCs induced by the translational diffusion of correlated molecules in the presence of pulsed field gradients should be different from those of SQCs. However, the diffusion effect on the iMQC signals resulting from intermolecular interactions is not yet well-understood.[13-16] In the prototype CRAZED sequence, which differs from the conventional pulsed gradient spin echo (PGSE) experiment, the molecular diffusion affects the evolution of the iMQCs during both the evolution period t_1 and detection period t_2. As described elsewhere, during the t_1 period, the multiple quantum coherences that correlate with the multi-spins from different molecules should evolve sensitively with the relaxation processes, susceptibility variations, and translational diffusion.[9,17,18] Additionally, during the t_2 period, diffusion could attenuate the strength of the distant dipolar field (or dipolar demagnetizing field), which is created by the modulated z-magnetization, and can convert the iMQCs into detectable signals, while there is no diffusional effect in the conventional PGSE experiment. Hence, the diffusion effect on the signal attenuation with the dipolar field should be considered for both the evolution and detection periods in the CRAZED-type experiments.

Previous studies have analytically revealed the diffusion effects on the iMQC signals for the limited condition.[13-16] In this paper, we analytically show the evolution behavior of an iMQC signal in a CRAZED-type sequence with molecular diffusion effects, and a comparison with numerical simulations conducted using various diffusion coefficients. To distinguish the diffusion effects during the t_1 and t_2 periods, the position of the first encoding gradient pulse was varied from the beginning to the end of the t_1 period. It should be noted that the other dynamics, except for the distant dipolar field (DDF) and diffusion, were ignored in the analytical and numerical calculations to clearly understand the effects of diffusion on the iMQC evolution.

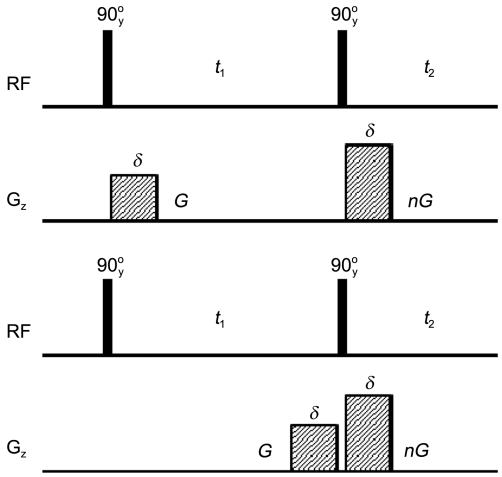

Figure 1. Two variations of the CRAZED pulse sequence depending on the position of the first encoding gradient pulse (top: at the beginning of the t_1 period; bottom: at the end the t_1 period).

In principle, both the quantum and classical treatments yield the same predictions for the iMQCs signal generated by intermolecular dipolar couplings in solution NMR. The quantum picture retains the individual dipolar couplings for all evolution periods and averages them at the end, while the classical picture averages all dipolar couplings first and then make evolution under that mean field.[3,17] For evaluating the diffusion effects, the classical approach would be suitable since the modified Bloch equation can easily incorporate the diffusion effects as well as the distant dipolar field.[2,19]

The Bloch equation, which modified to include the distant dipolar field and molecular diffusion process, can be written as[2,19]

$$\frac{d\mathbf{M}(\mathbf{r})}{dt} = \gamma\mathbf{M}(\mathbf{r}) \times \{\mathbf{B}(\mathbf{r}) + \mathbf{B}_d(\mathbf{r})\} + D\nabla^2\mathbf{M}(\mathbf{r}), \qquad (1)$$

where $\mathbf{M}(\mathbf{r})$ is the magnetization, $\mathbf{B}(\mathbf{r})$ is the applied magnetic field, $\mathbf{B}_d$ is the distant dipolar field, and D is the diffusion coefficient.

When we apply the first gradient pulse at the beginning of the t_1 period, we have to consider the diffusion effect on the modulated transverse magnetization during that period. After the second 90° pulse, which is followed by the evolution during t_1, the longitudinal and transverse magnetizations in

the rotating frame are, respectively,

$$M_z = -M_0\cos(\Delta\omega_0 t_1+\gamma G\delta z)\exp\{-D(\gamma G\delta)^2 t_1\}\,, \tag{2}$$

$$M^+ = M_x + iM_y$$
$$= iM_0\sin(\Delta\omega_0 t_1+\gamma G\delta z)\exp\{-D(\gamma G\delta)^2 t_1\}\,, \tag{3}$$

where $\Delta\omega_0$ is the resonance frequency in the rotating frame, γ is the gyromagnetic ratio, G is the gradient strength, and δ is the gradient duration. For simplicity, we assume that t_1 and t_2 are much longer than δ.

The second decoding gradient might select a specific coherence depending on the ratio of two gradients, n. For example, if n = 2, then only the SQCs, which were the intermolecular double quantum coherences (iDQCs) during the t_1 period, can pass through the gradient filter. If we consider the diffusion of the modulated longitudinal magnetization along z-axis and evolution of transverse magnetization under the distant dipolar field after the t_2 period, then

$$M_z = -M_0\cos(\Delta\omega_0 t_1+\gamma G\delta z)$$
$$\times\exp\{-D(\gamma G\delta)^2 t_1\}\exp\{-D(\gamma G\delta)^2 t_2\} \tag{4}$$

$$M^+ = M_x + iM_y$$
$$= iM_0\sin(\Delta\omega_0 t_1+\gamma G\delta z)\exp\{-D(\gamma G\delta)^2 t_1\}$$
$$\times\exp i\left[\begin{array}{l}\Delta\omega_0 t_2 + n\gamma G\delta - \\ \dfrac{1}{\tau_d}\displaystyle\int_0^{t_2}\cos(\Delta\omega_0 t_1+\gamma G\delta z)e^{-D(\gamma G\delta)^2 t_1}e^{-D(\gamma G\delta)^2 t}dt\end{array}\right]$$
$$= iM_0\sin(\Delta\omega_0 t_1+\gamma G\delta z)\exp\{-D(\gamma G\delta)^2 t_1\}$$
$$\times\exp i\left[\begin{array}{l}\Delta\omega_0 t_2 + n\gamma G\delta z-\cos(\Delta\omega_0 t_1+\gamma G\delta z)e^{-D(\gamma G\delta)^2 t_1} \\ \times\dfrac{1}{\tau_d D(\gamma G\delta)^2}\left\{1-e^{-D(\gamma G\delta)^2 t_2}\right\}\end{array}\right] \tag{5}$$

where $\displaystyle\int_0^{t_2}\exp\{-D(\gamma G\delta)^2 t\}dt = \frac{1}{D(\gamma G\delta)^2}\left(1-e^{-D(\gamma G\delta)^2 t_2}\right)$

and the dipolar demagnetizing time $\tau_d = (\gamma\mu_0 M_0)^{-1}$.[17]

For simplicity, let $D^* = D(\gamma G\delta)^2$. Using the Bessel J function formalism,

$$\exp(iz\cos x) = \sum_{m=-\infty}^{\infty} i^m J_m(z)\exp(imx)\,, \tag{6}$$

$$M^+ = iM_0\sin(\Delta\omega_0 t_1+\gamma G\delta z)\exp(-D^* t_1)\exp\{i(\Delta\omega_0 t_2+n\gamma G\delta z)\}$$
$$\times\sum_{m=-\infty}^{\infty}\left(\begin{array}{l}i^m J_m\left\{-\dfrac{\left(1-e^{-D^* t_2}\right)e^{-D^* t_1}}{\tau_d D^*}\right\} \\ \times\exp\{i(m\Delta\omega_0 t_1+m\gamma G\delta z)\}\end{array}\right)$$
$$= \frac{M_0}{2}\{e^{i(\omega_0 t_1+\gamma G\delta z)} - e^{-i(\omega_0 t_1+\gamma G\delta z)}\}$$
$$\times\exp(-D^* t_1)\exp\{i(\Delta\omega_0 t_2+n\gamma G\delta z)\}$$

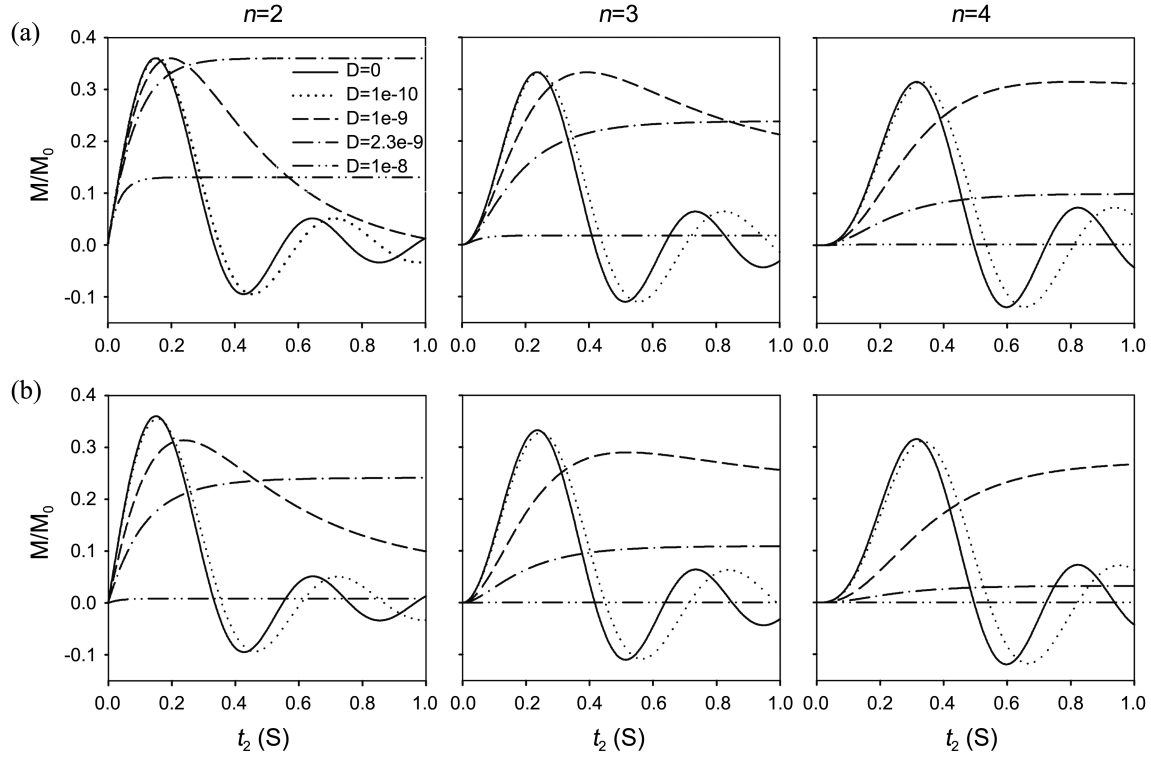

Figure 2. Calculated signal intensity profiles as a function of t_2 for diffusion coefficient variation samples based on the analytical solutions from (a) Eq. (10), and (b) Eq. (9). The gradient ratio, n, indicates multiple quantum coherence order, which can pass through the gradient filter, during the t_1 period. Note that the values of the diffusion coefficient D in the legends are shown in units of m^2/s.

$$\times \sum_{m=-\infty}^{\infty} \left(i^m J_m \left\{ -\frac{\left(1-e^{-D^* t_2}\right) e^{-D^* t_1}}{\tau_d D^*} \right\} \times \exp\{i(m\Delta\omega_0 t_1 + m\gamma G\delta z)\} \right). \quad (7)$$

To determine the effect of the spatial modulation of magnetization, we collect all the position dependent terms as,

$$\{\exp(i\gamma G\delta z) - \exp(-i\gamma G\delta z)\}\exp(in\gamma G\delta z) \sum_{m=-\infty}^{\infty} \exp(im\gamma G\delta z)$$

$$= \sum_{m=-\infty}^{\infty} [\exp\{i(m+n+1)\gamma G\delta z\} - \exp\{i(m+n-1)\gamma G\delta z\}]. \quad (8)$$

For the magnetization to be nonzero after spatial averaging over the sample, the position dependent term should be constant with respect to position. This means that the coefficient for the z-direction in Eq. (7) must be zero. Therefore, the condition of $m = -(n \pm 1)$ is required for a signal to exist.

Using the Bessel function relations $J_{-n}(x) = (-1)^n J_n(x)$ and $J_{n-1}(x) + J_{n+1}(x) = (2n/x)J_n(x)$, the observable magnetization can be expressed, after spatial averaging, as follows:

$$M^+ = i^{n-1} n M_0 \exp(i\Delta\omega_0 t_2)\exp(-in\Delta\omega_0 t_1) \times \frac{\tau_d D^*}{1-e^{-D^* t_2}} J_n\left\{ -\frac{\left(1-e^{-D^* t_2}\right) e^{-D^* t_1}}{\tau_d D^*} \right\}. \quad (9)$$

If we apply the first gradient pulse at the end of the t_1 period (Fig. 1), then we can only consider the diffusion effect during the acquisition period t_2. Therefore, Eq. (9) could be simplified as

$$M^+ = i^{n-1} n M_0 \exp(i\Delta\omega_0 t_2)\exp(-in\Delta\omega_0 t_1) \times \frac{\tau_d D^*}{1-e^{-D^* t_2}} J_n\left(-\frac{1-e^{-D^* t_2}}{\tau_d D^*} \right). \quad (10)$$

Figure 2 shows signal growth patterns along with t_2 depending on the diffusion coefficient values and the gradient ratio based on the analytical solutions, Eq. (9) and Eq. (10). The following parameter values for the pure water sample in a 600 MHz NMR spectrometer at 298 K were used for the analytical calculations and numerical simulations: $G = 10$ G/cm, $\delta = 2$ ms, $t_1 = 50$ ms, $\tau_d = 65.3$ ms. When diffusion is slow enough (*e.g.* $D \sim 10^{-10}$ m^2/s), it barely affects the signal intensity of the iMQCs even at high orders. While the signal growing profiles can be significantly altered by the diffusion effects with the actual value for pure water ($D = 2.3 \times 10^{-10}$ m^2/s), the self-diffusion coefficients of many organic solvents are similar to or less than that of water. Therefore, molecular diffusions could be an important factor for determining signal intensities of the iMQCs.

From the expansion of the Bessel function in Eqs. (9) and (10), it can be deduced that the iMQCs during the t_1 period are affected by molecular diffusion proportional to the quantum order (*i.e.* n). In the other word, the iMQCs during the t_1 period would decay exponentially at the rate of nD (if t_1 is short enough). Additionally, diffusion has an effect on the magnitude of the distant dipolar field during the acquisition period t_2 by decaying the amplitude of the modulated z-magnetization exponentially. Evaluating this effect might be complicated since the iMQCs signals grow with time t_2 in a manner different from the case of the conventional SQCs that decay with time. To make the iMQC signal sufficiently large for detection, a longer time evolution under the distant dipolar field is required depending on the coherence order, as shown in Figure 2. In quantum treatment, it corresponds to the time to strip up I_z operators by dipolar couplings in multi-spin single-quantum coherences (*e.g.* $I_{xi}I_{zj}I_{zk}$) to become detectable single-spin single-quantum coherences (I^+).[3,17,18] Consequently, the diffusion effect on the iMQCs should be quite different from, and greater than, that on the conven-

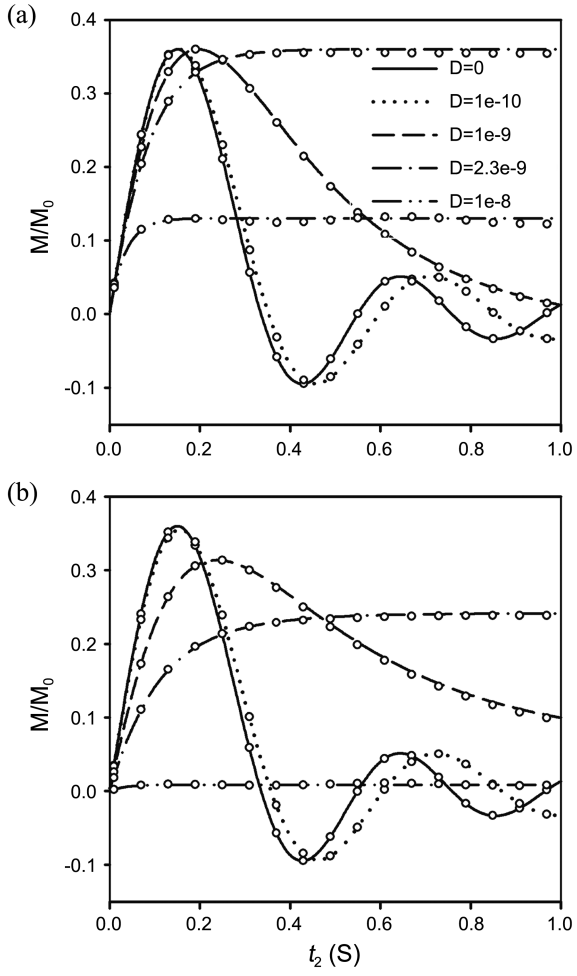

Figure 3. The comparison of the signal intensity profiles (for $n = 2$) using analytical calculations and numerical simulations that depends on the diffusion coefficients (a) without and (b) with diffusion effects during the t_1 period. The open circles indicate the results of numerical simulations with the same conditions as those of the corresponding analytical curves. Only a limited number of circles are shown for clarity.

tional SQC.

The signal profiles obtained through numerical simulation agree very well with those from the analytical calculations, as shown in Figure 3. This implies that the analytical calculation results, Eq. (9) and Eq. (10), could be appropriate solutions to explain diffusion effects on the iMQCs. In real experiments, the signal intensity behaviors of the iMQCs are influenced by other dynamics as well as diffusion. Hence, it would be difficult to evaluate the effects of diffusion separately. In this regard, the analytical solution could be meaningful when considering applications such as diffusion MRI. Note that the simulation was conducted by numerically integrating the modified Bloch equation (Eq. (1)) through the Cash-Karp Runge-Kutta method.[19]

In conclusion, we calculated the analytical solutions to evaluate the effects of diffusion on the iMQCs in CRAZED pulse sequences. The obtained solution has been verified using the results of numerical simulation. The diffusional behaviors of the iMQCs during both the evolution and detection time periods could be examined by the analytical solution, which was quite different from those of the conventional NMR experiments. Understanding the difference in diffusional behaviors could lead to useful applications such as diffusion MRI based on the detection of iMQCs.

Acknowledgments. This Research was supported by the Chung-Ang University Research Scholarship Grant in 2010 (DW).

References

1. Warren, W. S.; Richter, W.; Andreotti, A. H.; Farmer II, B. T. *Science* **1993**, *262*, 2005.
2. Bowtell, R.; Robyr, P. *Phys. Rev. Lett*. **1996**, *76*, 4971.
3. Ahn, S.; Warren, W. S.; Lee, S. *J. Magn. Reson.* **1997**, *28*, 114.
4. Cho, J. H.; Cho, J.; Chung, K.-C.; Yu, H.-Y.; Ryu, E. K.; Ahn, S.; Lee, C. *Bull. Korean Chem. Soc.* **2011**, *32*, 2113.
5. Marques, J. P.; Bowtell, R. *Magn. Reson. Med*. **2004**, *51*, 148.
6. Cai, C.; Gao, F.; Cai, S.; Huang, Y.; Chen, Z. *J. Magn. Reson.* **2011**, *211*, 162.
7. Warren, W. S.; Ahn, S.; Mescher, M.; Garwood, M.; Ugurbil, K.; Richter, W.; Rizi, R. R.; Hopkins, J.; Leigh, J. S. *Science* **1998**, *281*, 247.
8. Rizi, R. R.; Ahn, S.; Alsop, D. C; Garrett-Roe, S.; Mescher, M.; Richter, W.; Mitchell, D. M. D.; Leigh, J. S.; Warren, W. S. *Magn. Reson. Med*. **2000**, *43*, 627.
9. Cho, J. H.; Ahn, S.; Lee, C.; Hong, K. S.; Chung, K.-C.; Chang, S.-K.; Cheong, C.; Warren, W. S. *Magn. Reson. Imaging* **2007**, *25*, 626.
10. Lin, Y.; Gu, T.; Chen, Z.; Kennedy, S.; Jacob, M.; Zhong, J. *Magn. Reson. Med.* **2010**, *63*, 303.
11. Cho, J. H.; Hong, K. S.; Cho, J.; Chang, S.-K.; Cheong, C.; Lee, N. H.; Kim, H.; Warren, W. S.; Ahn, S.; Lee, C. *J. Magn. Reson.* **2012**, *217*, 86.
12. Shen, G.; Cai, C.; Chen, Z.; Cai, S. *Magn. Reson. Imaging* **2013**, *31*, 515.
13. Ardelean, I.; Kimmich, R. *J. Chem. Phys*. **2000**, *112*, 5275.
14. Chen, Z.; You, R.; Zhong, J. *J. Chem. Phys*. **2001**, *114*, 5642.
15. Barros, W., Jr.; Gore, J. C.; Gochberg, D. F. *J. Magn. Reson.* **2006**, *178*, 166.
16. Lin, T.; Sun, H.; Chen, Z.; You, R.; Zhong, *J. Magn. Reson. Imaging* **2007**, *25*, 1409.
17. Lee, S.; Richter, W.; Vathyam, S.; Warren, W. S. *J. Chem. Phys*. **1996**, *105*, 874.
18. Ahn, S.; Lee, S.; Warren, W. S. *Mol. Phys*. **1998**, *95*, 769.
19. Enss, T.; Ahn, S.; Warren, W. S. *Chem. Phys. Lett*. **1999**, *305*, 101.